mRNA was detected in oocytes and embryos, being relatively abundant during cleavage and blastula stages (Fig. 4A). TLF is widely expressed in the embryo, as was shown in a large-scale in situ hybridization screen using randomly picked cDNAs, one of which was TLF (clone 3.39) (*23*). We targeted the endogenous TLF mRNA for degradation with a DEED-modified oligonucleotide, TLF-AS93, similar to the way in which we targeted TBP mRNA with TBP-AS3. TLF-AS93 mediated efficient degradation of TLF mRNA in vivo (Fig. 4D). TLF-AS93–injected embryos developed normally until the onset of embryonic transcription between stage 8 and 9, the stage at which they arrested (Fig. 4, B and C). TLF-AS57, a different oligonucleotide capable of degrading TLF mRNA in vivo, caused a similar developmental arrest, whereas control oligonucleotides did not (*16*). Recently, a similar early embryonic arrest was observed in *tlf-1* (*RNAi*) embryos of *C. elegans* (*24*, *25*). We examined the expression of embryonically transcribed genes in TLF-AS93–injected embryos, and we could not detect embryonic transcription of *Xbra* or *EF1*α, and *GS17* RNA was also severely reduced [Fig. 4, D and E (*16*)]. Maternal TBP mRNA, which in normal embryos is translated at the MBT (*11*), was translated in TLF-AS93 embryos (Fig. 4D), albeit with slightly lower efficiency. We ruled out a possible contribution of lower TBP levels to the TLF-AS93 phenotype by overexpressing TBP with a synthetic TBP mRNA. Both the TLF-AS93–mediated developmental arrest and the transcriptional impairment of GS17 were independent of TBP levels (Fig. 4D). The expression of MyoD and GS17 was examined in more detail. In the absence of detectable amounts of TBP, MyoD was not transcribed de novo, although low levels of maternally deposited MyoD RNA were observed (Fig. 4E). In TLF-AS93–injected embryos, on the other hand, MyoD was expressed after their developmental arrest, most notably at the time normal embryos start gastrulation [stage 10 to 11 (Fig. 4E)]. GS17 expression by comparison was significantly affected in TLF-AS93 embryos (Fig. 4, D and E) but much less so in TBP-AS3 embryos (Figs. 3B and 4E).

These data establish that TBP is essential for transcription of some but not all class II and class III genes during early embryogenesis. TBP is dispensable for transcription of a subset of genes and for the onset of gastrulation, whereas it is required for sustaining embryonic development. TLF, on the other hand, is essential for development beyond the mid-blastula stage. Our analysis of TBP and TLF function suggests that a remarkable functional dichotomy exists regarding general transcription factor requirements. Important developmental genes such as *Xbra* are transcribed in the absence of TBP, whereas a gene such as *MyoD* is strictly TBP-dependent. TBP and TLF fulfill distinct requirements for transcription and embryogenesis.

### References and Notes


1. N. Hernandez, *Genes Dev.* **7**, 1291 (1993).
2. S. Takada, J. T. Lis, S. Zhou, R. Tjian, *Cell* **101**, 459 (2000).
3. M. C. Holmes, R. Tjian, *Science* **288**, 867 (2000).
4. J. C. Dantonel, J. M. Wurtz, O. Poch, D. Moras, L. Tora, *Trends Biochem. Sci.* **24**, 335 (1999).
5. M. Teichmann *et al.*, *Proc. Natl. Acad. Sci. U.S.A.* **96**, 13720 (1999).
6. P. A. Moore *et al.*, *Mol. Cell. Biol.* **19**, 7610 (1999).
7. M. D. Rabenstein, S. Zhou, J. T. Lis, R. Tjian, *Proc. Natl. Acad. Sci. U.S.A.* **96**, 4791 (1999).
8. J. Newport, M. Kirschner, *Cell* **30**, 675 (1982).
9. ———, *Cell* **30**, 687 (1982).
10. P. Bell, U. Scheer, *Exp. Cell Res.* **248**, 122 (1999).
11. G. J. C. Veenstra, O. H. J. Destrée, A. P. Wolffe, *Mol. Cell. Biol.* **19**, 7972 (1999).
12. M.-N. Prioleau, J. Huet, A. Sentenac, M. Méchali, *Cell* **77**, 439 (1994).
13. G. Almouzni, A. P. Wolffe, *EMBO J.* **14**, 1752 (1995).
14. J. M. Dagle, J. L. Littig, L. B. Sutherland, D. L. Weeks, *Nucleic Acids Res.* **28**, 2153 (2000).
15. J. M. Dagle, D. L. Weeks, *Methods Enzymol.* **313**, 420 (2000).
16. G. J. C. Veenstra, D. L. Weeks, A. P. Wolffe, data not shown.
17. J. C. Sible, J. A. Anderson, A. L. Lewellyn, J. L. Maller, *Dev. Biol.* **189**, 335 (1997).
18. J. Smith, *Trends Genet.* **15**, 154 (1999).
19. P. A. Krieg, D. A. Melton, *EMBO J.* **4**, 3463 (1985).
20. P. A. Krieg, S. M. Varnum, W. M. Wormington, D. A. Melton, *Dev. Biol.* **133**, 93 (1989).
21. M. Jamrich, T. D. Sargent, I. B. Dawid, *Genes Dev.* **1**, 124 (1987).
22. R. A. W. Rupp, H. Weintraub, *Cell* **65**, 927 (1991).
23. V. Gawantka *et al.*, *Mech. Dev.* **77**, 95 (1998).
24. J. C. Dantonel, S. Quintin, L. Lakatos, M. Labouesse, L. Tora, *Mol. Cell.* **6**, 715 (2000).
25. L. Kaltenbach, M. A. Horner, J. H. Rothman, S. E. Mango, *Mol. Cell.* **6**, 705 (2000).
26. Supplementary Web information on materials and methods is available on *Science* Online at www.sciencemag.org/cgi/content/full/290/5500/2312/DC1.


27. We thank T. D. Sargent for constructs, C. Greaves for synthesis of DEED-modified oligonucleotides, E. Schlag for sequencing, and I. B. Dawid and J. M. Dagle for helpful discussions. D.L.W. was supported by grants from NIH.

20 September 2000; accepted 21 November 2000


# Cholinergic Enhancement and Increased Selectivity of Perceptual Processing During Working Memory


**Maura L. Furey,[1]* Pietro Pietrini,[2] James V. Haxby[1]**



**Using functional magnetic resonance imaging, we investigated the mechanism by which cholinergic enhancement improves working memory. We studied the effect of the cholinesterase inhibitor physostigmine on subcomponents of this complex function. Cholinergic enhancement increased the selectivity of neural responses in extrastriate cortices during visual working memory, particularly during encoding. It also increased the participation of ventral extrastriate cortex during memory maintenance and decreased the participation of anterior prefrontal cortex. These results indicate that cholinergic enhancement improves memory performance by augmenting the selectivity of perceptual processing during encoding, thereby simplifying processing demands during memory maintenance and reducing the need for prefrontal participation.**


Working memory (WM) (*1*) is mediated by a widely distributed neural system in the human brain. Modulation of cholinergic neurotransmission alters memory function, including WM. Performance on WM tasks is improved by pharmacologic agents that enhance cholinergic function and is impaired by agents that block cholinergic function (*2–4*). The mechanism by which cholinergic modulation alters WM, however, is unclear.

Different regions in the distributed neural system for WM support dissociable cognitive subcomponents of this complex function. With functional magnetic resonance imaging (fMRI) the neural activity associated with WM can be decomposed into task subcomponents that are separated in time and space, namely the responses during perceptual encoding, activity during memory delays, and the responses during recognition testing (*5, 6*).

Prefrontal cortex plays a central role in maintaining and manipulating the contents of WM (*7, 8*), but previous work suggests this region is not the site where cholinergic enhancement improves processing efficiency. Cholinergically mediated improvement in WM performance is correlated with reduced activity in right prefrontal cortex (*9, 10*). Reduced activity in this region likely reflects reduced WM load or task difficulty (*11, 12*)


[1]Laboratory of Brain and Cognition, National Institute of Mental Health, National Institutes of Health, Bethesda, MD, USA. [2]Department of Human and Environmental Sciences, University of Pisa, Pisa, Italy.

*To whom correspondence should be addressed. E-mail: furey@nih.gov

**Table 1.** Effect sizes and the significances of differences between effect sizes during placebo and drug infusion in dorsal and ventral extrastriate regions. Effects are contrasts between responses to different subcomponents, expressed as differences in percent response: Nonselective = responses to visual stimuli minus responses to a blank screen; Face-selective = responses to faces minus responses to control stimuli; Encoding-selective = responses during face encoding minus responses during face retrieval; Memory delay = activity during the memory delays minus activity during the control delays. Asterisks indicate effects that were significantly altered by cholinergic enhancement: *, $P < 0.05$; **, $P < 0.01$.

| Response contrasts | Placebo | Drug |
|---|---|---|
| *Ventral occipital* | | |
| Nonselective | 0.97 | 0.94 |
| Face-selective | 0.60 | 0.87** |
| Encoding-selective | 0.39 | 1.13** |
| Memory delay | 0.35 | 0.22 |
| *Ventral temporal* | | |
| Nonselective | 0.62 | 0.69 |
| Face-selective | 0.59 | 0.74** |
| Encoding-selective | 0.69 | 0.88 |
| Memory delay | 0.14 | 0.19 |
| *Dorsal occipital* | | |
| Nonselective | 0.41 | 0.52* |
| Face-selective | 0.28 | 0.47* |
| Encoding-selective | 0.18 | 0.42* |
| Memory delay | −0.13 | 0.03 |
| *Intraparietal sulcus* | | |
| Nonselective | 0.27 | 0.26 |
| Face-selective | 0.39 | 0.47* |
| Encoding-selective | 0.33 | 0.43 |
| Memory delay | 0.07 | 0.10 |

that is a consequence of increased efficiency in other regions of the WM system.

Here, we show that cholinergic enhancement of WM is associated with increased selectivity of responses during perceptual processing in visual extrastriate cortices, particularly during encoding, and redistributed memory delay activity, suggesting that processing demands for WM maintenance were simplified by the production of a more robust visual percept during encoding.

Seven young healthy subjects participated in a double-blind, placebo controlled, crossover study with two fMRI sessions on separate days, one during a steady-state infusion of physostigmine and one during an infusion of saline (*13, 14*). During scanning, subjects performed a task that consisted of alternating face WM and sensorimotor control items (Fig. 1).

We measured cortical responses to different subcomponents of the task and identified voxels with significant responses to visual stimuli or significant memory delay activity (*5, 15*). Visual responses were classified as face-selective if the response to faces was greater than the response to control stimuli and were classified as encoding-selective if the response during face encoding was greater than the response during recognition testing.

**Table 2.** Effect of cholinergic enhancement on region volumes in ventral occipital, ventral temporal, and dorsal occipital cortices. For each region, the volumes ($cm^3$) of cortex (±SE) showing a significant overall experimental effect and the percent of the total combined region volumes (±SE) showing significant face-selective, encoding-selective, or memory delay effects are shown for each of the two experimental sessions. Total combined regions ($cm^3$) consisted of voxels that showed a significant overall experimental effect on either placebo or drug and were as follows: ventral occipital, 19.6 ± 3.3; ventral temporal, 20.2 ± 3.8; and dorsal occipital, 12.3 ± 4.1.

| Region volumes | Placebo | Drug |
|---|---|---|
| *Ventral occipital* | | |
| Total | 15.4 ± 2.6 | 15.4 ± 3.8 |
| Face-selective | 16.6 ± 3.6% | 25.9 ± 5.0% |
| Encoding-selective | 1.8 ± 1.9% | 6.4 ± 3.0% |
| Memory delay | 10.5 ± 2.9% | 18.3 ± 4.2% |
| *Ventral temporal* | | |
| Total | 13.8 ± 2.7 | 15.6 ± 3.8 |
| Face-selective | 12.6 ± 3.0% | 18.4 ± 2.9% |
| Encoding-selective | 1.5 ± 1.4% | 2.7 ± 2.4% |
| Memory delay | 6.1 ± 2.6% | 13.0 ± 3.4% |
| *Dorsal occipital* | | |
| Total | 9.7 ± 2.8 | 10.4 ± 3.3 |
| Face-selective | 7.4 ± 2.8% | 12.1 ± 3.0% |
| Encoding-selective | 2.5 ± 2.1% | 6.0 ± 2.8% |
| Memory delay | 6.5 ± 3.6% | 7.0 ± 3.8% |

Performance of this WM task during saline infusion evoked activity in a widely distributed, bilateral set of cortical regions (*16*). Figure 2 illustrates the locations of the posterior regions in one subject and shows the mean time series, averaged over subjects ($n = 7$, for all regions), hemispheres, and trials, during physostigmine and saline infusions. Table 1 shows the size of each of the effects of interest in these ventral and dorsal visual regions. The magnitude of each contrast was measured for the subset of voxels within each region that showed significance on that contrast during either session. The percentage of each posterior region that showed the response of interest is indicated in Table 2.

Infusion of physostimine resulted in enhanced neural processing in visual cortical areas and a trend toward faster reaction times (RT) ($P = 0.07$) during WM (*17*). In ventral occipital cortex (Fig. 2A and Table 1), both the face-selectivity and the encoding-selectivity of responses to stimuli were significantly enhanced by physostigmine ($P < 0.01$ in both cases), as indicated by larger differences between the responses to faces and control stimuli (face-selectivity) and between the responses during encoding and recognition testing (encoding-selectivity). Responses in ventral temporal cortex (Fig. 2B and Table 1) also showed significant enhancement of face-selectivity during physostigmine infusion ($P < 0.01$) and a nonsignificant trend toward enhanced encoding-selectivity ($P = 0.09$). Responses in dorsal extrastriate regions of occipital and parietal cortices were of smaller amplitude (compare Fig. 2, A and B, to Fig. 2, C and D) and involved smaller cortical volumes (Table 2) than those observed in ventral extrastriate cortices. Nonetheless, responses in dorsal occipital cortex (Fig. 2C and Table 1), like ventral occipital cortex, showed significant enhancement of both face-selectivity and encoding-selectivity during physostigmine infusion ($P < 0.05$ in both cases), and responses in the intraparietal sulcus (Fig. 2D and Table 1) showed significant enhancement of face-selectivity ($P < 0.05$). The increased face-selectivity of responses in ventral occipital cortex resulted from both an increased response to faces ($P < 0.05$) and a decreased response to control stimuli ($P < 0.05$), whereas increased face-selectivity in the other regions was due primarily to increased responses to faces.

Enhancement of visual processing by physostigmine also was evident as changes in the volume of cortex that showed significant selectivity or memory delay activity (Table 2)

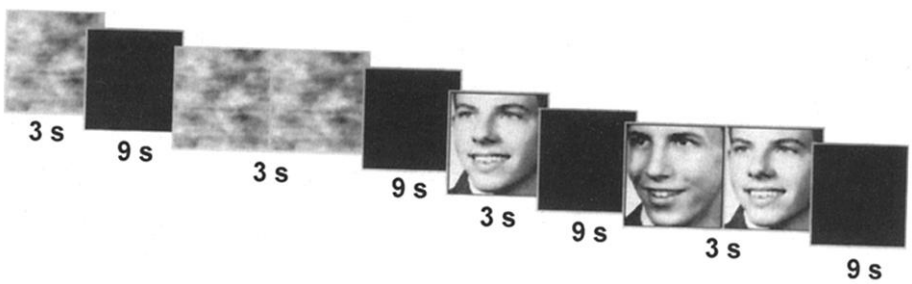


**Fig. 1.** The WM for faces task. For each scan series, subjects performed a task that alternated between a sensorimotor control item and a WM item. For each WM item, a picture of a face was presented for 3 s, followed by a 9-s delay, and by a 3-s presentation of two faces. Subjects indicated which of the two faces they had seen previously by pressing response buttons with the right or left thumb. For each sensorimotor control item, identical scrambled faces were presented in the same spatial and temporal manner as in the WM item. Scrambled faces were used to control for spatial frequency, brightness, and contrast. Subjects were informed that there was no memory component for this portion of the task and instructed to press both buttons simultaneously when shown two scrambled faces. Different scrambled faces were used across trials. Items were separated by 9-s intertrial intervals.

(*18*). The volume of cortex that showed face-selectivity increased by approximately 50% in ventral occipital, dorsal occipital, and ventral temporal cortex ($P < 0.05$). Similarly, the volume of cortex that showed encoding-selectivity increased over twofold in these same regions ($P < 0.05$). These changes were not due to a greater overall volume of activated cortex with physostigmine as the volume of cortex in visual areas that was activated by any component of the face WM task did not change ($P > 0.2$). The number of voxels in the ventral occipital and temporal cortices that showed significant memory delay activity increased nearly twofold with cholinergic enhancement ($P < 0.05$), despite the fact that the magnitude of sustained activity over memory delays in these voxels did not increase significantly (Table 1). The volumes of cortex in the intraparietal sulcus showing face-selectivity, encoding-selectivity, and memory delay activity did not change with cholinergic enhancement.

In prefrontal cortex, significant responses were observed bilaterally in the inferior frontal gyrus ($n = 4$), in the anterior and posterior middle frontal gyri ($n = 5$ and $n = 7$, respectively), and in the superior frontal gyrus ($n = 3$). These regions were bilateral in most cases. When unilateral, there were an equivalent number of right-sided ($n = 4$) and left-sided ($n = 3$) regions. Physostigmine induced a reduction of activity during WM in dorsal anterior prefrontal regions (anterior middle frontal and superior frontal gyri, defined by voxels that showed significant memory delay activity, $P < 0.01$) that was not specific to individual subcomponents but was a general effect across the WM task. By contrast, physostigmine induced a similarly nonspecific increase of activity during WM ($P < 0.05$) in the inferior prefrontal cortex. In the posterior middle frontal region, physostigmine had no effect on activity during WM task performance. Thus, enhanced processing during physostigmine infusion is associated with reduced participation of dorsal anterior but not inferior prefrontal regions.

The results indicate that enhancement of cholinergic activity improves WM by focusing perceptual processing in extrastriate visual areas on relevant stimuli, particularly during encoding. The difference between responses to memory and control visual stimuli increased in both ventral and dorsal visual extrastriate cortices, with larger increases during encoding. Cholinergic enhancement also increased the volume of cortex showing memory delay activity in ventral extrastriate cortex, although there was no significant effect on the amplitude of memory delay activity. Consistent with our previous findings (*9*), activity during perceptual processing and

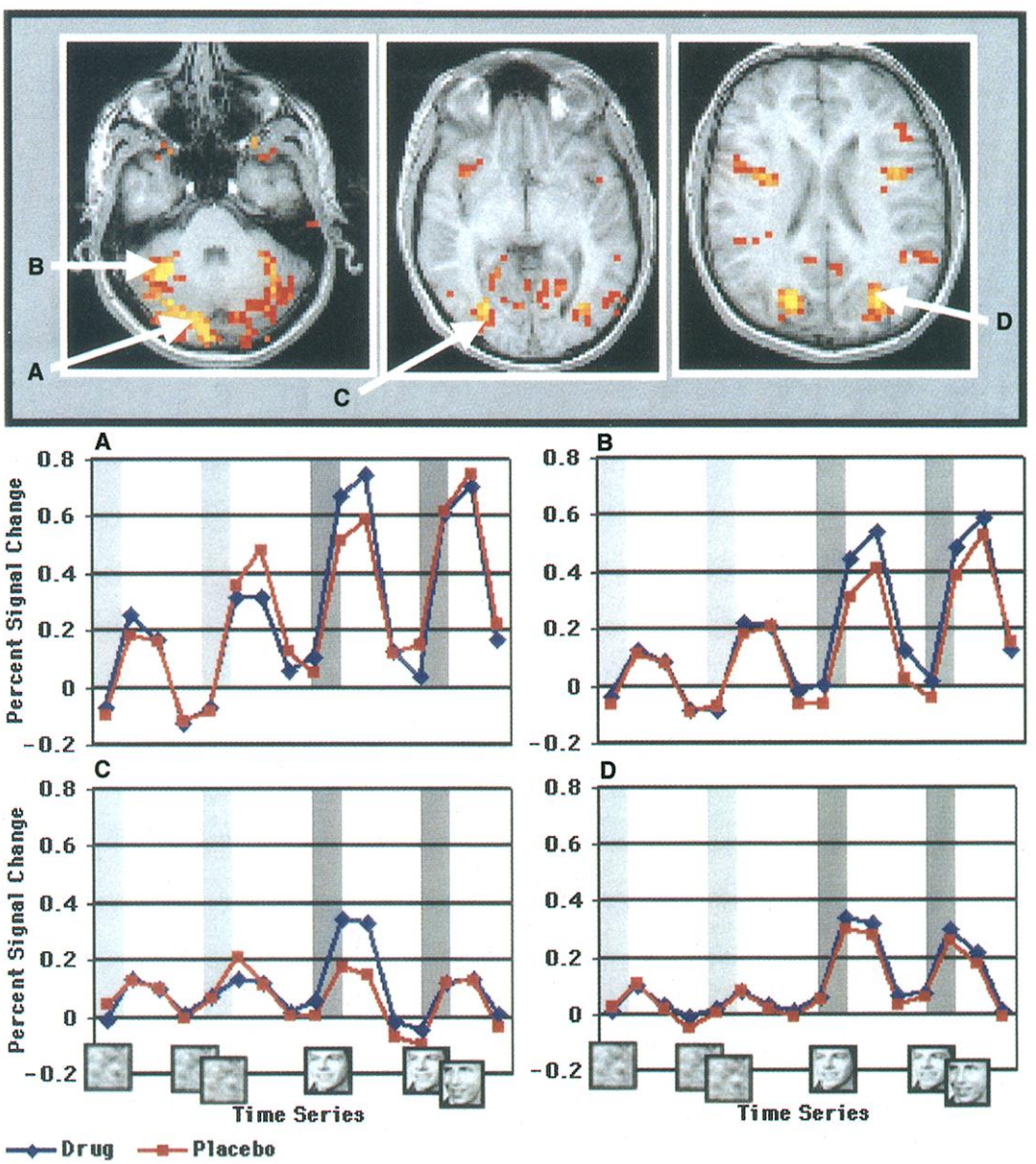


**Fig. 2.** Examples of ventral and dorsal extrastriate visual areas that were activated in the WM task and time series data from the two experimental sessions. Three axial slices from a single representative subject are shown at the top of the figure with the voxels that showed a significant response to any component of the WM task shown in color. Arrows indicate the locations of ventral occipital (**A**), ventral temporal (**B**), dorsal occipital (**C**), and intraparietal (**D**) regions. The four panels on the bottom of the figure show time series averaged across subjects, hemispheres, and all trials for the voxels that showed significant face-selectivity [(A), (B), and (D)] or encoding-selectivity (C). The figures show percent change in signal from baseline. The light gray bars indicate when the control stimuli (scrambled faces) were presented and the dark gray bars illustrate when the memory stimuli (faces) were presented. Data acquired during placebo (red) and during physostigmine (blue) are shown in each panel.

memory maintenance in dorsal anterior prefrontal cortex was reduced during cholinergic enhancement.

Cholinergic modulation is known to influence the signal-to-noise ratio for the responses of single neurons in cortex (*19, 20*). We demonstrated this effect at a cortical systems level, by the increased face-selectivity and encoding-selectivity of neural responses during physostigmine infusion. Signal-to-noise ratio can be improved by increasing signal or by decreasing noise. Our data show increased responses to memory stimuli (i.e., signal), and, in early visual processing areas, decreased responses to control stimuli (i.e., noise; Fig. 2A).

Cholinergic projections of the nucleus basalis of Meynert to the neocortex influence visual attention (*21, 22*). In single-unit recording studies, enhanced selective attention is demonstrated as an enhanced tuning of neural responses to attended stimuli (*23*). In a single-unit study in cats, cholinergic enhancement augmented the selectivity of visual neurons to stimulus orientation (*24*). In functional imaging studies the effect of selective attention is evident as increased responses in extrastriate visual areas that process the attended information (*25, 26*). Our results indicate that cholinergic enhancement augments selective attention, as evidenced by increased selectivity of perceptual responses. Our results do not identify the mechanism by which attention is modulated. Cholinergic neurotransmission could influence selective attention through a direct effect on systems that control attention or by modulating the effect of input from the control systems on local neural activity in perceptual areas. Specific cellular mechanisms have been suggested (*20*) by which acetylcholine could modulate the effect of input from attention control systems by increasing the response to afferent input and reducing background activity. Because the effect of physostigmine infusion was an increase in the selectivity of responses to task-relevant stimuli rather than increased responses to all stimuli, our results indicate that the effect of cholinergic enhancement is not a simple increase in alertness or arousal.

Cholinergic enhancement of perceptual processing has a greater effect on memory at the time of encoding than at the time of retrieval. Consistent with this finding, cholinergic antagonists, such as scopolamine, selectively interfere with encoding of new information, but not with retrieval (*27–29*).

Cholinergic enhancement also redistributed sustained activity during memory delays. In prefrontal cortex, memory delay activity was reduced in dorsal anterior regions and increased in inferior regions. In ventral extrastriate cortex, the volume of cortex that showed significant memory delay activity doubled. Enhanced encoding could account for this redistribution of memory delay activity. Improved encoding can produce a more vivid or distinct visual percept that is easier to maintain in WM as a simple image, mediated by activity in ventral temporal and inferior frontal cortex, as opposed to a representation that requires more executive function to construct and maintain, mediated by activity in dorsal anterior prefrontal cortex (*30*). Alternatively, cellular mechanisms have been proposed by which cholinergic input could increase sustained neural firing directly (*31*).

Deterioration of the cholinergic system contributes to memory failure and cognitive decline in Alzheimer's disease and also may play a role in the more benign memory changes associated with healthy aging (*32, 33*). The main pharmacological agents used to counteract cognitive dysfunction in patients with Alzheimer's disease are cholinesterase inhibitors, similar to physostigmine but with a longer plasma half-life (*34*). Our results suggest that the enhancement of memory performance induced by these cholinergic agents is mediated primarily by more selective perceptual processing during encoding.

### References and Notes


1. A. Baddeley, R. Logie, S. Bressi, S. Della Sala, H. Spinnler, *Q. J. Exp. Psychol.* **38**, 603 (1986).
2. A. J. Glasky, C. L. Melchior, B. Pirzadeh, N. Heydari, R. F. Ritsmann, *Pharmacol. Biochem. Behav.* **47**, 325 (1994).
3. G. R. Dawson, S. D. Iverson, *Behav. Brain Res.* **57**, 143 (1993).
4. T. W. Robbins *et al.*, *Psychopharmacology* **134**, 95 (1997).
5. S. M. Courtney, L. G. Ungerleider, K. Keil, J. V. Haxby, *Nature* **386**, 608 (1997).
6. J. D. Cohen *et al.*, *Nature* **386**, 604 (1997).
7. S. Funahashi, C. J. Bruce, P. S. Goldman-Rakic, *J. Neurophysiol.* **61**, 331 (1989).
8. G. Rainer, W. F. Asaad, E. K. Miller, *Proc. Natl. Acad. Sci. U.S.A.* **95**, 15008 (1998).
9. M. L. Furey *et al.*, *Proc. Natl. Acad. Sci. U.S.A.* **94**, 6512 (1997). Physostigmine and other cholinesterase inhibitors enhance cholinergic function by prolonging the action of endogenously released acetylcholine.
10. M. L. Furey *et al.*, *Brain Res. Bull.* **51**, 213 (2000).
11. T. S. Braver *et al.*, *Neuroimage* **5**, 49 (1997).
12. C. L. Grady *et al.*, *Hum. Brain Mapp.* **4**, 227 (1996).
13. All participants (two male, five female) gave written informed consent. Gradient echo, echo planar imaging (repetition time 3 s, echo time 40 ms, flip angle 90) was used on a GE Signa 1.5-T scanner (Milwaukee, WI). Whole-brain volumes, composed of 24 contiguous, 5-mm-thick, axial slices, were obtained in 12 series of 92 scans as each subject performed the WM for faces and control tasks. All subjects received an intravenous infusion of physostigmine at a rate of 1 mg/hour according to the following procedure: A 10-min loading dose (1.93 mg/hour) to quickly achieve desired blood plasma levels, followed by a maintenance drip (0.816 mg/hour) to maintain stable drug levels to completion of the study. Infusions continued for 30 min before the beginning of the task to obtain stable drug effects (*14*). To minimize peripheral side effects, glycopyrrolate (0.2 mg) was given intravenously before the physostigmine infusion. Glycopyrrolate is a cholinergic antagonist that does not cross the blood-brain barrier, and thus acts as a peripheral blocker of physostigmine effects. The same infusion schedule was used with saline on the placebo infusion day. Blood pressure and ECG were monitored throughout the study on both days in all subjects.
14. M. L. Furey *et al.*, *Pharmacol. Biochem. Behav.* **66**, 475 (2000).
15. Time series data were analyzed on a voxel-by-voxel basis using multiple regression (*5, 35*), and were done separately for the two experimental days for each subject. Hemodynamic delays were estimated on a voxel-by-voxel basis from the time series data based on a Fourier analysis of the phase delays of the principal frequencies in the experimental paradigm. Regressors in the multiple regression model were designed to identify responses to different subcomponents within the experimental design: (i) the response during face encoding, (ii) activity during the memory delay, (iii) the response during recognition memory testing, (iv) the response to the scrambled stimulus at the beginning of control items, (v) activity during the control item delay, (vi) the response to the pair of scrambled pictures that ended each control item, (vii) the intertrial interval that preceded each memory item, and (viii) the intertrial interval that preceded each control item. Selected contrasts between responses to different subcomponents were calculated as effects of interest: (i) responses to visual stimuli minus responses to a blank screen (nonselective visual response), (ii) responses to faces (including both encoding and recognition testing stimuli) minus responses to control stimuli (face-selective visual response), (iii) the response during face encoding minus the response during face retrieval (encoding-selective visual response), and (iv) activity during the memory delay minus activity during the control delay (memory delay activity). Regions of interest were defined as those showing a significant signal change ($Z > 4.0$, $P < 0.0001$) for the overall experimental effect with a minimum of five contiguous significant voxels. Within these regions showing a significant overall experimental effect, subregions were identified that had significant contrasts for the individual effects of interest ($Z > 3.09$, $P < 0.001$). Mean echoplanar brain scans from each experimental session were created and registered to a location midway between the locations of the scans in their original image volumes. Maps of the regions of interest from the two scanning sessions were resampled into this common reference frame. The same regions from the two sessions were combined to create a single region in the common space that contained all voxels that showed a significant effect on either day. Thus, these regions were defined in a way that was not biased toward greater effects for either day. These significance maps were superimposed onto a structural MRI for each individual subject to identify their anatomical locations (*16*). Mean time series associated with these regions of interest were determined for each subject and for each experimental session. Multiple regression then was performed on each individual region of interest time series to calculate the magnitude of the effects of interest as differences in percent signal change (nonselective visual, face-selective, encoding-selective, and activity during the memory delay). Contrast magnitudes were analyzed using repeated measures ANOVA (analysis of variance) to test the significance of changes in response contrasts between placebo and drug sessions.
16. Regions of interest were defined as voxels showing significant effects (*15*) in the following locations, as defined by anatomical landmarks that were identified on structural MRI scans (with Talairach coordinates of mean center of gravity): ventral occipital cortex including the lateral occipital sulcus, the inferior occipital gyrus and inferior part of the middle occipital gyrus, and the posterior part of the fusiform gyrus (left −24, −77, and −14; right 18, −79, and −15); ventral temporal cortex including the inferior and fusiform gyri (left −28, −52; and −12; right 27, −55, and −16); dorsal occipital cortex including the superior occipital gyrus and the intraoccipital sulcus (left −32, −72; and 12, right 26, −74, and 12); intraparietal sulcus (left −28, −60; and 31, right 28, −59, and 31); inferior prefrontal cortex including the inferior frontal gyrus and anterior insular cortex (left −31, 40, and 1; right 39, 38, and −4); anterior middle frontal gyrus (left -27, 39, and 26; right 36, 39, and 21); posterior middle frontal gyrus (left −41, 11, and

23; right 36, 13, and 27); superior frontal gyrus (left −9, 31, and 45; right 17, 35, and 37).

17. Although the improvement in WM performance with cholinergic enhancement was a nonsignificant trend in the current study ($P = 0.07$), in a previous study (*9*) with a larger sample ($n = 13$) the effect was highly significant ($P < 0.001$). In the current study, we analyzed RT data for six of our seven subjects because the behavioral data for one subject were unavailable due to a computer failure. The difference in the significance of the two findings is simply a result of the difference in sample sizes. A power analysis shows that the size of the RT difference and variability in the current sample would yield a significant result ($P = 0.01$) with a sample size of 13. During the memory trials, mean RT was 1180 ms during placebo and 1119 ms during physostigmine. During the control trials, mean RT was 735 ms during placebo and 709 ms during physostigmine, a difference that did not approach significance ($P = 0.24$), suggesting that the effect of cholinergic enhancement on WM performance is not due to a nonspecific increase in arousal.
18. Matched-pair *t* tests (two-tailed) were used to test the significance of drug-related changes in the volume of regions of interest that showed significant response contrasts.
19. H. Sato, Y. Hata, H. Masui, T. Tsumoto, *J. Neurophysiol.* **55**, 765 (1987).
20. M. E. Hasselmo, *Behav. Brain Res.* **67**, 1 (1995).
21. M. G. Baxter, A. A. Chiba, *Curr. Opin. Neurobiol.* **9**, 178 (1999).
22. B. J. Everitt, T. W. Robbins, *Annu. Rev. Psychol.* **48**, 649 (1997).
23. R. Desimone, J. Duncan, *Annu. Rev. Neurosci.* **18**, 193 (1995).
24. P. C. Murphy, A. M. Sillito, *Neuroscience* **40**, 13 (1991).
25. M. Corbetta, F. M. Miezin, S. Dobmeyer, G. L. Shulman, S. E. Peterson, *J. Neurosci.* **11**, 2383 (1991).
26. J. V. Haxby *et al.*, *J. Neurosci.* **14**, 6336 (1994).
27. A. Rosier, L. Cornette, G. A. Orban, *Neuropsychobiology* **37**, 98 (1998).
28. M. E. Hasselmo, B. P. Wyble, G. V. Wallenstein, *Hippocampus* **6**, 693 (1996).
29. S. P. Mewaldt, M. M. Ghoneim, *Pharmacol. Biochem. Behav.* **10**, 1205 (1979).
30. M. Petrides, *Philos. Trans. R. Soc. London Ser. B* **351**, 1455 (1996).
31. M. E. Hasselmo, E. Fransen, C. Dickson, A. A. Alonso, *Ann. N.Y. Acad. Sci.* **911**, 418 (2000).
32. M. M. Mesulam, *Prog. Brain Res.* **109**, 285 (1996).
33. R. T. Bartus, R. L. Dean III, B. Beer, A. S. Lippa, *Science* **217**, 408 (1985).
34. N. Qizilbash *et al.*, *JAMA* **280**, 1777 (1998).
35. J. V. Haxby, J. Ma. Maisog, S. M. Courtney, in *Mapping and Modeling the Human Brain*, P. Fox, J. Lancaster, K. Friston, Eds. (Wiley, New York, in press).
36. We express our appreciation to S. Courtney, R. Desimone, Y. Jiang, S. Kastner, L. Latour, A. Martin, L. Pessoa, and L. Ungerleider for careful and critical review of the manuscript. We also thank M. B. Schapiro and S. I. Rapoport for input during early stages of this project. This research was supported by the National Institute on Mental Health and National Institute on Aging Intramural Research Programs.

7 August 2000; accepted 15 November 2000

# A Global Geometric Framework for Nonlinear Dimensionality Reduction

**Joshua B. Tenenbaum,[1]* Vin de Silva,[2] John C. Langford[3]**

**Scientists working with large volumes of high-dimensional data, such as global climate patterns, stellar spectra, or human gene distributions, regularly confront the problem of dimensionality reduction: finding meaningful low-dimensional structures hidden in their high-dimensional observations. The human brain confronts the same problem in everyday perception, extracting from its high-dimensional sensory inputs—30,000 auditory nerve fibers or $10^6$ optic nerve fibers—a manageably small number of perceptually relevant features. Here we describe an approach to solving dimensionality reduction problems that uses easily measured local metric information to learn the underlying global geometry of a data set. Unlike classical techniques such as principal component analysis (PCA) and multidimensional scaling (MDS), our approach is capable of discovering the nonlinear degrees of freedom that underlie complex natural observations, such as human handwriting or images of a face under different viewing conditions. In contrast to previous algorithms for nonlinear dimensionality reduction, ours efficiently computes a globally optimal solution, and, for an important class of data manifolds, is guaranteed to converge asymptotically to the true structure.**

A canonical problem in dimensionality reduction from the domain of visual perception is illustrated in Fig. 1A. The input consists of many images of a person's face observed under different pose and lighting conditions, in no particular order. These images can be thought of as points in a high-dimensional vector space, with each input dimension corresponding to the brightness of one pixel in the image or the firing rate of one retinal ganglion cell. Although the input dimensionality may be quite high (e.g., 4096 for these 64 pixel by 64 pixel images), the perceptually meaningful structure of these images has many fewer independent degrees of freedom. Within the 4096-dimensional input space, all of the images lie on an intrinsically three-dimensional manifold, or constraint surface, that can be parameterized by two pose variables plus an azimuthal lighting angle. Our goal is to discover, given only the unordered high-dimensional inputs, low-dimensional representations such as Fig. 1A with coordinates that capture the intrinsic degrees of freedom of a data set. This problem is of central importance not only in studies of vision (*1*–*5*), but also in speech (*6*, *7*), motor control (*8*, *9*), and a range of other physical and biological sciences (*10*–*12*).

[1]Department of Psychology and [2]Department of Mathematics, Stanford University, Stanford, CA 94305, USA. [3]Department of Computer Science, Carnegie Mellon University, Pittsburgh, PA 15217, USA.

*To whom correspondence should be addressed. E-mail: jbt@psych.stanford.edu

The classical techniques for dimensionality reduction, PCA and MDS, are simple to implement, efficiently computable, and guaranteed to discover the true structure of data lying on or near a linear subspace of the high-dimensional input space (*13*). PCA finds a low-dimensional embedding of the data points that best preserves their variance as measured in the high-dimensional input space. Classical MDS finds an embedding that preserves the interpoint distances, equivalent to PCA when those distances are Euclidean. However, many data sets contain essential nonlinear structures that are invisible to PCA and MDS (*4*, *5*, *11*, *14*). For example, both methods fail to detect the true degrees of freedom of the face data set (Fig. 1A), or even its intrinsic three-dimensionality (Fig. 2A).

Here we describe an approach that combines the major algorithmic features of PCA and MDS—computational efficiency, global optimality, and asymptotic convergence guarantees—with the flexibility to learn a broad class of nonlinear manifolds. Figure 3A illustrates the challenge of nonlinearity with data lying on a two-dimensional "Swiss roll": points far apart on the underlying manifold, as measured by their geodesic, or shortest path, distances, may appear deceptively close in the high-dimensional input space, as measured by their straight-line Euclidean distance. Only the geodesic distances reflect the true low-dimensional geometry of the manifold, but PCA and MDS effectively see just the Euclidean structure; thus, they fail to detect the intrinsic two-dimensionality (Fig. 2B).

Our approach builds on classical MDS but seeks to preserve the intrinsic geometry of the data, as captured in the geodesic manifold distances between all pairs of data points. The crux is estimating the geodesic distance between faraway points, given only input-space distances. For neighboring points, input-space distance provides a good approxima-